

Bacterial RNA virus MS2 exposure increases the expression of cancer progression genes in the LNCaP prostate cancer cell line

SWAPNIL GANESH SANMUKH^{1,3}, NILTON JOSÉ DOS SANTOS^{1,4}, CAROLINE NASCIMENTO BARQUILHA^{1,4}, MÁRCIO DE CARVALHO⁵, PATRICIA PINTOR DOS REIS⁵, FLÁVIA KARINA DELELLA¹, HERNANDES F. CARVALHO⁴, DOROTA LATEK³, TAMÁS FEHÉR² and SÉRGIO LUIS FELISBINO¹

¹Laboratory of Extracellular Matrix Biology, Department of Structural and Functional Biology, Institute of Biosciences of Botucatu, Sao Paulo State University, Botucatu, São Paulo 18618-689, Brazil;

²Synthetic and Systems Biology Unit, Biological Research Center, Eötvös Loránd Research Network, 6726 Szeged, Hungary;

³Faculty of Chemistry, University of Warsaw, 02-093 Warsaw, Poland; ⁴Department of Structural and Functional Biology, Institute of Biology, University of Campinas, Campinas, São Paulo 13083-970; ⁵Department of Surgery and Orthopedics, Faculty of Medicine, Sao Paulo State University, Botucatu, São Paulo 18618-687, Brazil

Received September 17, 2022; Accepted December 2, 2022

DOI: 10.3892/ol.2023.13672

Abstract. Bacteriophages effectively counteract diverse bacterial infections, and their ability to treat most types of cancer has been explored using phage engineering or phage-virus hybrid platforms. In the present study, it was demonstrated that the bacteriophage MS2 can affect the expression of genes associated with the proliferation and survival of LNCaP prostate epithelial cells. LNCaP cells were exposed to bacteriophage MS2 at a concentration of 1×10^7 plaque forming units/ml for 24–48 h. After exposure, various cellular parameters, including cell viability, morphology, and changes in gene expression, were examined. MS2 affected cell viability adversely, reducing viability by 25% in the first 4 h of treatment; however, cell viability recovered within 24–48 h. Similarly, the *AKT*, androgen receptor, integrin $\alpha 5$, integrin $\beta 1$, *MAPK1*, *MAPK3*, *STAT3*, and peroxisome proliferator-activated receptor- γ coactivator 1 α genes, which are involved in various normal cellular processes and tumor progression,

were significantly upregulated, whereas the expression levels of *HSP90*, *ITGB5*, *ITGB3*, *HSP27*, *ITGAV*, and *PI3K* genes were unchanged. Therefore, based on viability and gene expression changes, bacteriophage MS2 severely impaired LNCaP cells by reducing anchorage-dependent survival and androgen signaling. A caveolin-mediated endocytosis mechanism for MS2-mediated signaling in prostate cancer cells was proposed based on reports involving bacteriophages T4, M13, and MS2, and their interactions with LNCaP and PC3 cell lines.

Introduction

In men, prostate cancer (PCa) is the second leading cause of death worldwide (1,2). Early detection and diagnosis are the most important steps to possibly curing PCa before it metastasizes (3,4). Different treatment modalities are important due to the resistance of cancer cells to chemo- and antiandrogenic therapies in advanced stages of the disease (5–7). With recent developments in the field of oncolytic and phage-based cancer therapies, there is a growing interest in novel approaches for cancer treatment. Recently, bacteriophages have been considered alternative nanoparticles for targeting, recognizing, and even killing cancer cells through phage engineering or adeno-associated virus/phage hybrids (8). Numerous research groups worldwide have reported the development of various phages, such as M13, MS2, T4, and T7, and have studied their important applications (9–18). MS2 virus-like particles (VLPs) can carry cargoes of small interfering RNA (siRNA) and modified RNA in the presence of specific nucleic acids, which makes them an ideal vehicle for targeted therapeutic drug delivery and imaging (11). In breast cancer, bacteriophage MS2 RNA-free capsids have been conjugated with anti-EGFR antibodies to target upregulated receptors using *in vitro* and *in vivo* models (12). In addition to its production efficiency, safety and non-toxicity, an MS2 VLP-based messenger RNA vaccine against PCa induced potent humoral and cell-mediated immune responses and slowed tumor growth, thus showing

Correspondence to: Professor Sérgio Luis Felisbino, Laboratory of Extracellular Matrix Biology, Department of Structural and Functional Biology, Institute of Biosciences of Botucatu, Sao Paulo State University, 250 Antônio Celso Wagner Zanin, Botucatu, São Paulo 18618-689, Brazil
E-mail: sergio.felisbino@unesp.br

Abbreviations: AR, androgen receptor; FGF, fibroblast growth factor; GPCR, G-protein coupled receptor; HSP27, heat shock protein 27; HSP90, heat shock protein 90; ITGA5, integrin $\alpha 5$; ITGAV, integrin αV ; ITGB1, integrin $\beta 1$; ITGB3, integrin $\beta 3$; ITGB5, integrin $\beta 5$; miR, microRNA; PFU, plaque forming unit; PGC1A, peroxisome proliferator-activated receptor- γ coactivator 1 α .

Key words: androgen receptor, gene expression, integrin, bacteriophage, MS2

promising results (13). Considering its *in vivo* safety, the bacteriophage MS2-L2 VLP has been used for oral immunization against various oral and vaginal human papillomavirus infections as well as head and neck, and cervical cancer (14). Similarly, VLPs are used to target abnormal cells *in vivo* by targeting surface peptides, e.g., a single chain fragment variable that binds to cell surface receptors [such as androgen receptors (ARs) or G protein-coupled receptors (GPCRs)] can be modified (15). In addition, nanovectors, such as MS2 VLPs, are used to target cancer cells for personalized therapy and to deliver anticancer components, such as siRNAs or long non-coding RNAs, for chemotherapy, immunotherapy, and radiotherapy; in this process, these VLPs interfere with RNA expression in cancer cells (16,17). MS2 bacteriophages target tumor tissues through internalizing Arg-Gly-Asp (RGD) motif peptides, which are ligands of integrins, and are used for the targeted delivery of apoptosis-inducing agents, such as thallium (I) nitrate (TINO₃ or NO₃Tl) and thallium (I) ions (Tl⁺) in tumor tissues (18). Since these agents penetrate bacteriophage MS2 particles and bind to their RNA molecules without inducing any side effects, they are particularly effective for clinical applications (18).

Based on our previously reported work with PC3 and LNCaP cells and their interactions with T4 and M13 phage (19-23); we found that LNCaP cells more closely represent metastasis Prostate cancer than PC3 cells due to their androgen independence. Hence, we selected LNCaP cells for MS2 phage interaction studies. Hence in the present study, key findings relating to the interaction of the natural bacteriophage, MS2, with the PCa cell line, LNCaP, were reported. Considering the importance of bacteriophages for natural phage therapy and previous reports of the interaction of T4 and M13 bacteriophages with PCa cell lines (PC3 and LNCaP) affecting cell migration and viability and modulating genes for cancer progression (19-23), the present study is of great importance to understand the direct effects of bacterial RNA viruses on PCa cell progression. Their effects on cell viability and genes that are involved in cancer cell proliferation [such as *AR*, *AKT*, *PI3K*, *MAPK1*, *MAPK3*, heat shock protein 90 (*HSP90*), heat shock protein 27 (*HSP27*), and peroxisome proliferator-activated receptor- γ coactivator 1 α (*PGC1A*)], and adhesion, migration, and invasion [such as integrins; integrin α 5 (*ITGA5*), integrin α V (*ITGAV*), integrin β 1 (*ITGB1*), integrin β 3 (*ITGB3*) and integrin β 5 (*ITGB5*)] were investigated. The results suggested that treatment affects cell metabolism and renders LNCaP cells dependent on AR/SRC signaling and AKT, and fibroblast growth factor (FGF)/MAPK signaling pathways, which can be easily treated with drugs, suggesting the possibility of using phages in combination therapies.

Materials and methods

LNCaP cell culture. LNCaP cells (ATCC CRL-1740) were obtained from American Type Culture Collection. The cell culture protocol was as described previously (23). Cells were grown in a 25-cm² culture flask (Qiagen, Inc.) containing RPMI 1640 medium (Gibco; Thermo Fisher Scientific, Inc.) supplemented with 10% FBS (Gibco; Thermo Fisher Scientific, Inc.), 50 μ g/ml penicillin, 50 μ g/ml streptomycin and 0.5 μ g/ml amphotericin B (Gibco; Thermo Fisher Scientific, Inc.), and

were incubated in 5% CO₂ in a CO₂ incubator at 37°C until 70% confluency. The cells were maintained in standard culture conditions (37°C, 5% CO₂ and 95% relative humidity). Cells were treated with 0.05% trypsin (Gibco; Thermo Fisher Scientific, Inc.) for 5 min at 37°C to detach the cells from the flask surface and transferred to a new 75-cm² culture flask (Qiagen, Inc.). During the experiment, the medium was changed every 2 days, and the cells were observed daily with an inverted microscope (Zeiss AG). Once cells reached 90% confluency, they were treated with 0.05% trypsin and transferred to new culture flasks or 24-well culture plates (Corning, Inc.) for hematoxylin and eosin staining, MS2 phage treatments, and cell viability experiments.

LNCaP cell exposure to bacteriophage MS2. Bacteriophage MS2 (ZeptoMetrix[®], LCC) was recovered at a concentration of 5.0x10¹⁰ plaque forming units (pfu)/ml in pre-made SM buffer (Thermo Fisher Scientific, Inc.) according to the manufacturer's instructions. Phages were not grown in bacterial culture due to possible contamination with nucleic acids, lipopolysaccharides, or endotoxins. Phages were centrifuged at 10,000 x g for 30 min at 4°C and then filtered through a 0.22- μ m cellulose acetate membrane filter (MilliporeSigma). The resulting phage cells were further diluted in a cell culture medium to reach 1x10⁷ pfu/ml (20-23) for LNCaP cancer cell treatment at 37°C for 24-48 h. This dilution series reduced trace impurities (including endotoxins) from the manufacturer-supplied stock solution (20-23).

MTT reduction assay. The LNCaP cells (5x10⁴) were seeded in 24-well plates. When the cells reached 70% confluence, they were treated with bacteriophage MS2 (10⁷ pfu/ml). After 4, 24, and 48 h of exposure, cell viability was determined using the MTT [3-(4,5-dimethylthiazol-2-yl)-2,5-diphenyltetrazolium bromide] (MilliporeSigma) reduction method according to the manufacturer's instructions (24,25). The resulting purple formazan was dissolved in 200 μ l of dimethyl sulfoxide. The reaction was performed in a 96-well plate and read using a spectrophotometer (Asys Hitech GmbH; Harvard Bioscience, Inc.) at 550 nm to determine the percentage of cell viability relative to control cells.

Hematoxylin and eosin staining. LNCaP cells were grown in 12-well plates with coverslips, as previously described in the LNCaP cell culture subsection. After reaching 30% confluency, LNCaP cells were exposed to vehicle PBS or bacteriophage MS2 treatment at 30°C at the highest concentration of 1x10⁷ pfu/ml for 24 and 48 h, washed with PBS, and fixed with 10% formaldehyde in PBS for 30 min at 30°C. The cells were then washed with PBS and stained with 1% hematoxylin (3-5 min) and 1% eosin (10 min) at room temperature. Coverslips were dried in ethanol, and the samples were mounted on glass slides using Permount[™] (Thermo Fisher Scientific, Inc.) and observed using a Leica light DMLB microscope (Leica Microsystems GmbH).

RNA extraction and cDNA synthesis for reverse transcription-quantitative PCR (RT-qPCR). LNCaP cells were treated with the bacteriophage MS2 at a concentration of 1x10⁷ cells at 37°C for 24 h. For total RNA extraction, the culture medium

Table I. Primers used for reverse transcription-quantitative PCR.

Genes	Forward primers (5'-3')	Reverse primers (5'-3')
<i>ACTB</i>	GATTCCTATGTGGGCGACGA	TGTAGAAGGTGTGGTGCCAG
<i>AKT</i>	CATCGCTTCTTTGCCGGTATC	ACTCCATGCTGTCATCTTGGTC
<i>AR</i>	GACATGCGTTTTGGAGACTGC	CAATCATTCTGCTGGCGCA
<i>GAPDH</i>	GAATGGGCAGCCGTTAGGAA	ATCACCCGGAGGAGAAATCG
<i>HSP90</i>	AGGGGGAAAGGGGAGTATCT	ATGTCAACCCTTGGAGCAGC
<i>HSP27</i>	CGCGGAAATACACGCTGCC	GACTCGAAGGTGACTGGGATG
<i>ITGA5</i>	GGGTGGTGTCTGTCTACCTC	GTGGAGCGCATGCCAAGATG
<i>ITGAV</i>	AGGCACCCTCCTTCTGATCC	CTTGGCATAATCTCTATTGCCTGT
<i>ITGB1</i>	GCCAAATGGGACACGCAAGA	GTGTTGTGGGATTTGCACGG
<i>ITGB3</i>	CTGCCGTGACGAGATTGAGT	CCTTGGGACACTCTGGCTCT
<i>ITGB5</i>	GGGCTCTACTCAGTGGTTTCG	GGCTTCCGAAGTCCTCTTTG'
<i>MAPK1</i>	TCAGCTAACGTTCTGCACCG	ACTTGGTGTAGCCCTTGGGA'
<i>MAPK3</i>	ATCTTCCAGGAGACAGCACG	TTCTAACAGTCTGGCGGGAG'
<i>PGC1A</i>	GAAGGGTACTTTTCTGCCCTT	CTTCTTCCAGCCTTGGGGAG'
<i>PI3K</i>	AGAGCCCCGAGCGTTT	TCGTGGAGGCATTGTTCTGA
<i>STAT3</i>	GCTTCTGCAAGAGTCAATG	TGTAGAAGGCGTGATTCTTCCC

ACTB, actin β ; *AR*, androgen receptor; *HSP27*, heat shock protein 27; *HSP90*, heat shock protein 90; *ITGA5*, integrin $\alpha 5$; *ITGAV*, integrin αV ; *ITGB1*, integrin $\beta 1$; *ITGB3*, integrin $\beta 3$; *ITGB5*, integrin $\beta 5$; *PGC1A*, peroxisome proliferator-activated receptor- γ coactivator 1 α .

was aspirated, and the cells were washed with PBS. Total RNA was extracted using an AllPrep DNA/RNA/protein extraction kit (Qiagen, Inc.) according to the manufacturer's instructions. Extracted total RNA was quantified using a NanoVue™ instrument (GE Healthcare). Finally, 2 μ g total RNA was reverse transcribed using the High-Capacity RNA-to-cDNA™ kit (Thermo Fisher Scientific, Inc) in a 20 μ l reaction according to the manufacturer's instructions.

Power SYBR™ Green/ROX qPCR 2X Master Mix (Applied Biosystems; Thermo Fisher Scientific, Inc.) was used for qPCR. The total reaction volume per sample was 10 μ l [5.0 μ l Power SYBR Green, 0.8 μ l (800 nM) of each forward and reverse oligonucleotide (Table I), 3.2 μ l nuclease-free water, 1 μ l cDNA] and was performed in triplicate in 384-well plates. The reaction was performed in a QuantStudio™ 12K Flex thermal cycler (Applied Biosystems; Thermo Fisher Scientific, Inc.) and the results were analyzed using the QuantStudio™ 12K Flex Real-Time PCR System v1.1 (Applied Biosystems; Thermo Fisher Scientific, Inc.). The reaction consisted of the following cycles: Step 1, 50°C for 2 min and 95°C for 2 min; step 2, 95°C for 1 sec and step 3, 60°C for 30 sec; steps 2 and 3 were repeated 40 times; dissociation curve with incubation at 95°C for 15 sec and 60°C for 1 min followed by a temperature gradient from 60 to 95°C at a rate of 0.15°C per sec.

The $2^{-\Delta\Delta Cq}$ method was used to calculate gene expression (26). This is based on the exponential PCR reaction, according to the formula $QR=2^{-\Delta\Delta Cq}$, where QR represents the level of gene expression, Cq represents the amplification cycle in which each sample undergoes exponential amplification, ΔCq refers to the difference between the Cq of the amplified sample for the target gene and the Cq of the same amplified sample for the reference gene, and $\Delta\Delta Cq$ represents the difference between the ΔCq of the sample of interest at a given time

point and the ΔCq of the reference sample. Fold change was calculated using $2^{-\Delta\Delta Cq}$, and the \log_2 fold change ($\log_2 FC$) was calculated. The results are presented as the $\log_2 FC$.

Reactions were performed using *GAPDH* as an endogenous control in triplicate for 14 target genes: *ACTB*, *AKT*, *AR*, *HSP27*, *HSP90*, *ITGA5*, *ITGAV*, *ITGB1*, *ITGB3*, *ITGB5*, *MAPK1*, *MAPK3*, *PGC1A*, and *PI3K*, using an ABI 7900 Real-Time PCR System (Applied Biosystems; Thermo Fisher Scientific, Inc.) according to the manufacturer's instructions. Values for all samples were normalized to the ratio between the target gene and mean Cq obtained for the reference gene *GAPDH*. The forward and reverse primers used are listed in Table I.

Bioinformatic analysis. The Enrichr (<https://maayanlab.cloud/Enrichr/>) gene set knowledge discovery server was used to predict gene ontology-based predictions for GO biological processes and GO cellular component prediction (27), to support evaluation of the association between gene expression and cancer cell progression. The STRING functional protein association server (<https://string-db.org/>) was used to assess protein-protein interaction through gene expression associated with cancer cell signaling protein pathways (28). The network of protein-protein interactions in *Homo sapiens* was constructed using the string protein-protein interaction network v11.5, using upregulated genes in LNCaP cells (based on gene expression results) for studying their protein-protein interactions with highest confidence level setting. Interactions of proteins were mapped using the highest confidence cut-off (0.7-0.9). In the resulting protein association network, proteins were presented as nodes connected by lines with varying thicknesses representing the highest confidence level (0.7-0.9).

Statistical analysis. Results are presented as mean \pm standard deviation or percent survival in graphs with at least three replicates. The Shapiro-Wilk normality test was used to test for normal data distribution. For results that passed the test, the Mann-Whitney test was used whereas for those which did not pass the normality test, Dunn's multiple comparison test was used. The unpaired t-test was performed to determine the significance of the results obtained. All statistical analyses were performed using GraphPad Prism (version 5.00; GraphPad Software, Inc.). $P < 0.05$ was considered to indicate a statistically significant difference.

Results

Cell morphology. LNCaP cells exposed to bacteriophage MS2 at 1×10^7 pfu/ml showed no marked morphological changes at 24 h compared with untreated cells. In particular, no spindle-shaped nucleus formation was observed following the staining of LNCaP cells treated with MS2 phages. Similarly, no marked morphological changes were observed after 48 h of exposure to the bacteriophage MS2 (Fig. 1).

MTT reduction assay to measure cell viability. Exposure to MS2 transiently reduced PCa cell viability. The MS2 bacteriophage exposure initially affected the viability of prostate cancer cells as compared with the cells treated with MS2 phages for 4, 24, and 48 h, they temporarily reduced the viability of LNCaP cells by 25% after 4 h of treatment. The cell viability was measured at 4, 24, and 48 h for control and phage-treated cells. Data are presented as percentages relative to untreated control cells at each time point. The bacteriophage MS2 didn't affect the viability at 24 and 48 h of exposure. After 24 and 48 treatments, no significant difference in the viability of LNCaP cells was noted (Fig. 2).

Gene expression profiles after exposure to bacteriophage MS2. Gene expression analysis of LNCaP cells after exposure to the bacteriophage MS2 revealed that some integrin genes were upregulated. After 24 h of exposure to bacteriophage MS2, the *ITGA5* and *ITGB1* genes showed significantly increased gene expression compared with untreated cells. Similarly, MS2 treatment significantly increased the expression levels of *AKT*, *AR*, *MAPK1*, *MAPK3*, *PGC1A*, and *STAT3*. Furthermore, important cancer progression-related genes, such as *HSP27*, *HSP90*, *ITGAV*, *ITGB3*, *ITGB5*, and *PI3K*, were not significantly affected by bacteriophage MS2 treatment of LNCaP cells (Fig. 3).

Bioinformatic analysis. The bioinformatics analysis based on upregulated genes was performed by using Enrichr (<https://maayanlab.cloud/Enrichr/>) gene set knowledge discovery server to predict gene ontology-based predictions for GO biological processes and GO cellular component prediction (27). The STRING functional protein association server was also used to understand the association and co-regulation of proteins expressed by these overexpressed genes through protein-protein interactions studies. We predicted 'caveolin-mediated endocytosis' (P-value: 0.000001399; Fig. S1) as a potential MS2 bacteriophage entry pathway from upregulated genes in LNCaP cells (27). Similarly for

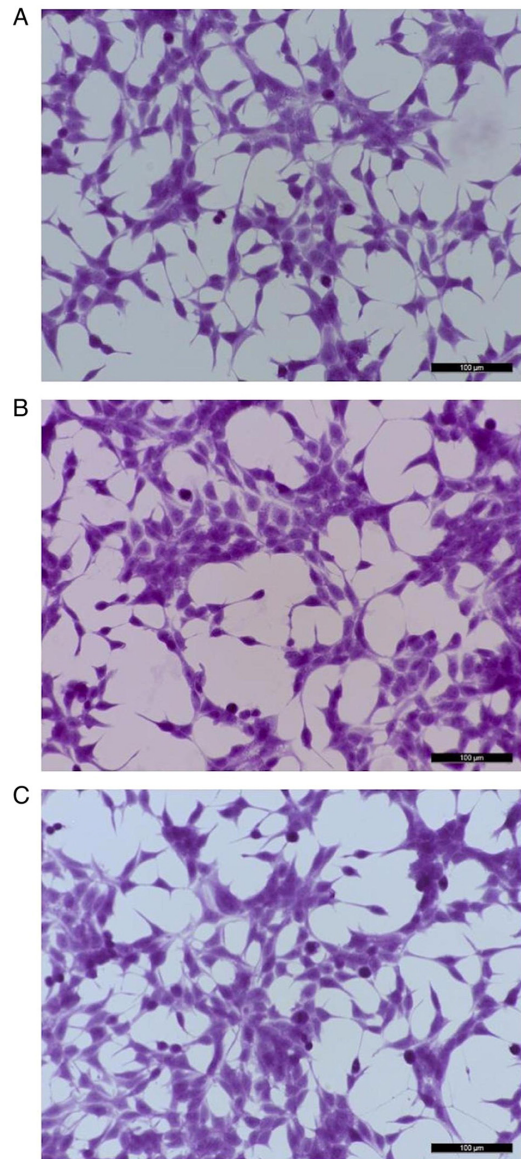


Figure 1. Representative images of LNCaP cells stained with hematoxylin-eosin. (A) Control (untreated LNCaP cells). (B) LNCaP cells after exposure to 1×10^7 pfu/ml of bacteriophage MS2 for 24 h. (C) LNCaP cells after exposure to 1×10^7 pfu/ml bacteriophage MS2 for 48 h. No marked morphological differences were observed between the treated and untreated cells even after 48 h of exposure to bacteriophage MS2. Scale bars, 100 μm .

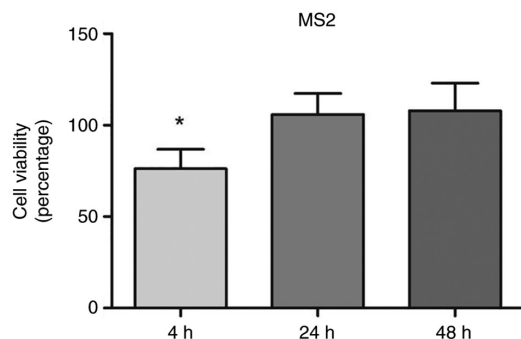


Figure 2. Viability of the LNCaP prostate cancer cells after 4, 24, and 48 h of exposure to 10^7 pfu/ml of MS2 bacteriophage. A significant reduction was observed after 4 h of incubation with MS2. Data are presented as percentages relative to untreated control cells at each time point. * $P < 0.05$ compared with the control group within the same observation period by unpaired t-test.

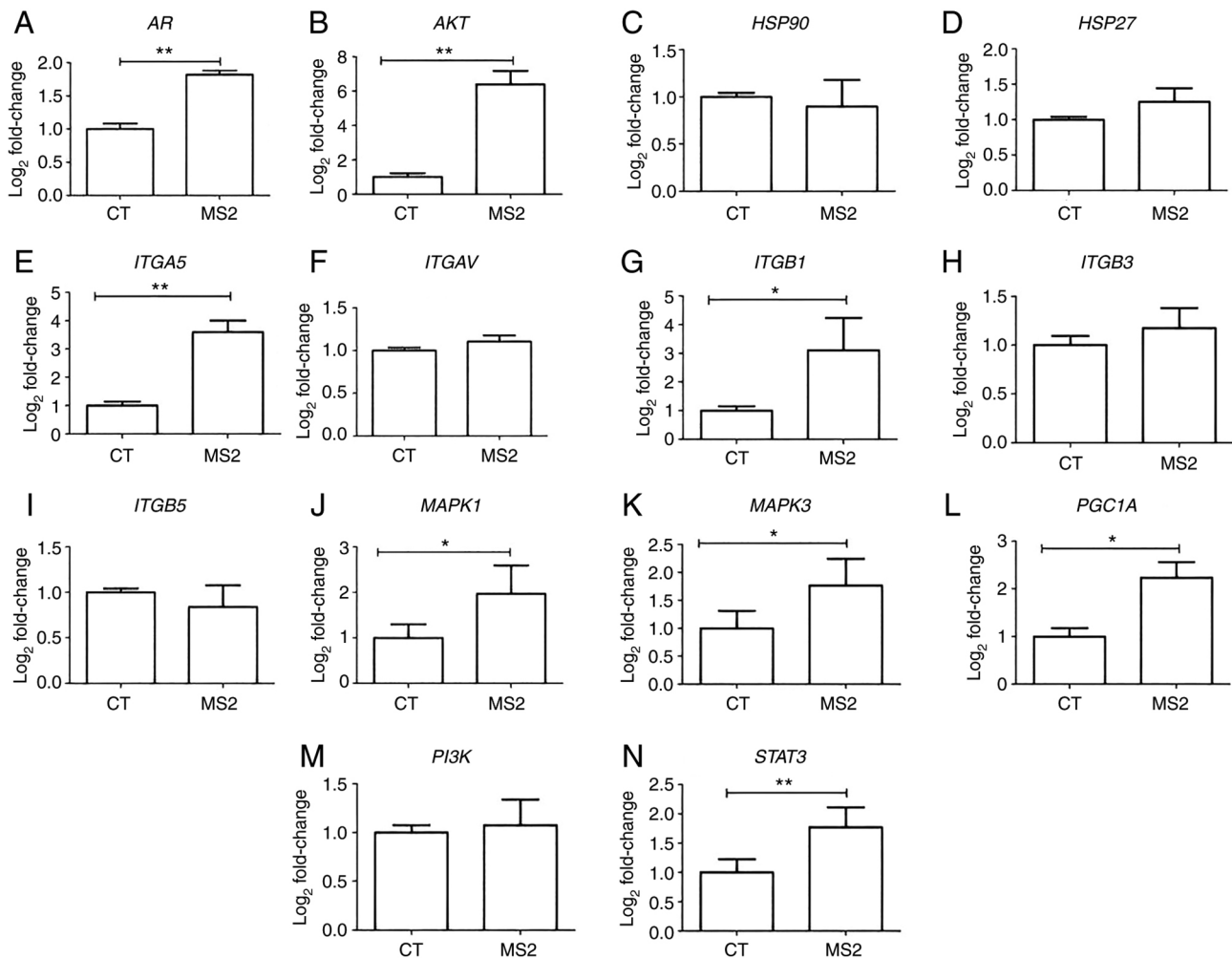


Figure 3. Gene expression of the LNCaP prostate cancer cells after 24 h of treatment with bacteriophage MS2. The effect on the gene expression of LNCaP cells after interaction with bacteriophage MS2 was compared with that of untreated CT cells. (A) *AR*, (B) *AKT*, (C) *HSP90*, (D) *HSP27*, (E) *ITGA5*, (F) *ITGAV*, (G) *ITGB1*, (H) *ITGB3*, (I) *ITGB5*, (J) *MAPK1*, (K) *MAPK3*, (L) *PGC1A*, (M) *PI3K*, and (N) *STAT3*. Relative values of gene expression (median) are shown as Log₂Fold-Change. *P<0.05 and **P<0.01 vs. control group within the same observation period, as determined using the non-parametric Kruskal-Wallis test. AR, androgen receptor; CT, control; *HSP27*, heat shock protein 27; *HSP90*, heat shock protein 90; *ITGA5*, integrin $\alpha 5$; *ITGAV*, integrin αV ; *ITGB1*, integrin $\beta 1$; *ITGB3*, integrin $\beta 3$; *ITGB5*, integrin $\beta 5$; *PGC1A*, peroxisome proliferator-activated receptor- γ coactivator 1 α .

bacteriophages T4 and M13, ‘integrin-mediated signaling pathway’ (P-value: 0.000007588) and ‘caveolin-mediated endocytosis’ (P-value: 0.000001799; Fig. S1) were predicted. Also, through GO cellular component prediction focal adhesion, cell-substrate junction, caveola, plasma membrane raft, early and late endosomes were predicted for MS2, T4, as well as M13 phages validating the caveolin-mediated endocytosis for these phages.

Discussion

Cellular receptors, including ARs, integrins, β -arrestins, and GPCRs, are key players in tumor growth, angiogenesis, and metastasis, and are indirectly regulated by phage-cancer cell interactions, which are involved in regulating numerous cellular functions, including proliferation, survival, and mortality (19–23). Furthermore, since numerous GPCRs (e.g., VPAC1 and VPAC2) serve as valuable biomarkers for cancer screening, inhibition of GPCRs may offer opportunities to develop novel mechanism-based strategies for cancer prevention and treatment (29). As different adhesion GPCRs

are differentially regulated during cancer progression, their role in different types of cancer is yet to be defined, and thus, requires further research (29,30). G protein-coupled receptor kinases (GRKs) and arrestins are involved in the regulation of intracellular signal transductions associated with different GPCRs and control various cellular processes (29,30). For example, GRKs 1–7 serves a role in regulating various stages of cancer progression and physiological processes, such as insulin resistance and inflammation (29,30).

Molecular dynamic simulations have enabled the development of rational anticancer peptides (ACPs), which improved the understanding of their interaction with different targets through protein-protein binding (31). The US Food and Drug Association and the European Medicines Agency have approved several ACPs for clinical use; however, for ACPs to be effective, they should overcome limitations associated with short plasma half-lives, degradation by proteinases, stability and immunogenicity (8–17,31,32). Expression of anticancer peptides/tumor targeting peptides/tumor-specific internalizing peptides are possible by presenting them on bacteriophage surfaces through the modification of coat protein genes (32).

It can increase the stability of the bound peptides and further enhance the interactions of engineered phages with GPCR receptor/integrins and other surface proteins/receptors to facilitate the understanding of their interaction between the different signaling pathways of the transmembrane receptor/proteins (32,33).

In the present study, it was observed that the interaction of LNCaP cells with bacteriophage MS2 did not markedly affect cell morphology or spindle formation. Similar observations were made after bacteriophages T4 and M13 interacted with LNCaP cells at different time intervals and phage concentrations as they altered the cancer progression-related gene expression, viability and cell migration (21,23). Regardless of whether phages affect the cytoskeleton of cancer cells, phages can be internalized and affect cancer cell signaling through various pathways (34,35). Similarly, in the present study, the interaction of bacteriophage MS2 with LNCaP cells affected cancer cell viability at different time intervals; however, viability was significantly affected only up to 4 h, and viability was restored after 24 and 48 h. These observations also fit well with those for bacteriophages T4 and M13 (23). Therefore, phage size and structure may have differential effects on the proliferation, migration, and viability of LNCaP cancer cells as reported previously (20-23). Also, bacteriophage MS2 impairs cell viability for 4 h as demonstrated during the present study. In addition, cell-penetrating peptides displayed on the bacteriophage M13, such as HIV-1 transactivator protein-derived TAT peptide, can enter live mammalian breast cancer cells and are destroyed within 2 h, which is also consistent with a previous viability study (35).

AR upregulation has been linked to the upregulation of estrogen receptor β , and *AR* is responsible for the activation of the Raf1-MEK signaling pathway, leading to MAPK activation (36). Similarly, the activation of *AR* can promote the activation of *AKT* metabolism, leading to the activation of mTOR (37,38), since overexpression of *AR* was associated with upregulation of *AKT* as observed in the present study demonstrated by the elevated gene expression of *AR* and *AKT* following MS2 phage exposure. Membrane-bound GPCRs also respond to androgen, which may increase apoptosis and phosphorylation of ERK and decrease cell migration and metastasis (20-23,39). In addition, *AR* regulates *SRC* expression via microRNA (miR)-203, prostate epithelial cell proliferation via miR-221, proliferation and viability via miR-96, migration, metastasis, and invasion via miR-541 and apoptosis via miR-125b by controlling the expression of genes, such as kallikrein-related peptidase 3 and prostate-specific membrane antigen, two important markers of prostate differentiation (39-42). Zhang *et al.* (42) demonstrated the delivery of microRNA-21-sponge and pre-microRNA-122 by MS2 virus-like particles to target hepatocellular carcinoma cells. In a previous study, the semi-adherent relative upsurge method, a simple gap-filling method to study the migration of adherent and semi-adherent cancer cells, was used to investigate the effects of bacteriophages T4 and M13 on androgen-dependent (LNCaP) and androgen-independent (PC3) cancer cell lines (20-23). The migration of these cancer cells was strongly influenced by the type of phage involved in the interaction experiments (21,22).

In the present study, *AR*, *AKT*, *MAPK1* and *MAPK3*, and other crucial genes, such as *ITGA5*, *ITGB1*, *PGC1A*, and *STAT3*, were significantly upregulated compared with the levels in the untreated control groups after 24 h of treatment with bacteriophage MS2 in LNCaP cells. Based on the upregulated gene profile in LNCaP cells, mechanisms by which LNCaP cells can activate survival mechanisms can be predicted. Considering the difference in gene expression patterns in LNCaP and PC3 cells concerning integrins, *ARs*, *AKT*, *HSPs*, *MAPKs*, *PGC1A* and *PI3K*, following the interaction between bacteriophages T4 and M13, it is clear that not only phage size, phage concentration and/or the exposure time, but also natural peptide display and genomic makeup affect the migration, viability and gene expression of cancer cells in cancer progression (20-23). In addition, since phage internalization is now a well-established concept (38), it was hypothesized that the effect of the phage genetic nature is also an important factor in altering cancer progression genes in both LNCaP and PC3 cells, as reported previously (Tables II and III) (19,21,22).

Viral entry is mediated by different modes depending on the virus type (34,35), and VLPs are used to deliver various drug molecules for therapeutic applications (43). Similarly, MS2 VLPs enter mammalian cells via caveolin-1-mediated ITGB1 endocytosis and alter gene expression (44). Caveolin-1 mRNA and protein are upregulated in metastatic murine and human PCa cells, and caveolin-1 internalization mediates integrin-dependent signaling pathways (44,45). MS2 is also taken up by mammalian cells using such pathways (44-46). Therefore, the present study is beneficial for understanding the impact of bacterial viruses, which make up the majority of the human microbiome, on cancer progression as well as bacteriophage therapies in humans.

Considering these variations, the protein-protein interaction map shown in Fig. 4 can be proposed for the co-regulation of cancer progression genes in LNCaP cells after interaction with bacteriophage MS2 (47). Similarly, the protein-protein interaction map for the co-regulation of cancer genes in LNCaP cells after interaction with bacteriophages T4 and M13, which were reported previously, is shown in Fig. S2 (20,22,23,47). From these interactions, it appears that the genetic nature of these phages (DNA or RNA), which is independent of the natural phage presentation by T4, M13, and MS2, also influences LNCaP cancer cell signaling. *SRC*, a proto-oncogenic tyrosine-protein kinase (or non-receptor protein tyrosine kinase), interacts with most of these proteins, and its activation involves various cellular receptors, including immune receptors, integrin bound to the extracellular matrix, adhesion receptors, platelet-derived growth factor receptor, GPCRs and cytokine receptors (39). The initial interaction of phages with various cellular transmembrane proteins facilitates internalization and modification of cancer progression gene expression by the phage genome, as reported previously (Fig. 5) (35,39).

Additionally, *ITGA5* and *ITGB1* are considered fibronectin receptors and potential targets for solid tumor treatment, as their upregulation is associated with poor prognosis in colon, breast, ovarian, lung, and brain tumors (47). Since $\alpha5\beta1$ recognizes and adheres to extracellular ligands containing the tripeptide arginine-glycine-aspartate motif, it can interact with numerous extracellular matrix molecules, such as VEGFR-1, fibrinogen, fibronectin, and fibrillin (48,49). In addition,

Table II. Effect of bacteriophages T4, M13 and MS2 separately on the expression of cancer progression genes in LNCaP and PC3 cells.

First author/s, year	Interacting bacteriophage	Cancer progression gene	LNCaP	PC3	(Refs.)	
Sanmukh <i>et al</i> , 2018; Sanmukh <i>et al</i> , 2021	T4 phage	<i>AKT</i>	Upregulated	Upregulated	(21,22)	
Sanmukh <i>et al</i> , 2018; Sanmukh <i>et al</i> , 2021		<i>AR</i>	Downregulated	Downregulated	(21,22)	
Sanmukh <i>et al</i> , 2017; Sanmukh <i>et al</i> , 2018; Sanmukh <i>et al</i> , 2021		<i>HSP90</i>	No alteration	Downregulated	(19,21,22)	
Sanmukh <i>et al</i> , 2018; Sanmukh <i>et al</i> , 2021		<i>HSP27</i>	No alteration	Downregulated	(21,22)	
Sanmukh <i>et al</i> , 2018; Sanmukh <i>et al</i> , 2021		<i>ITGA5</i>	Upregulated	Upregulated	(21,22)	
Sanmukh <i>et al</i> , 2018; Sanmukh <i>et al</i> , 2021		<i>ITGAV</i>	No alteration	Upregulated	(21,22)	
Sanmukh <i>et al</i> , 2018; Sanmukh <i>et al</i> , 2021		<i>ITGB1</i>	Upregulated	No alteration	(21,22)	
Sanmukh <i>et al</i> , 2018; Sanmukh <i>et al</i> , 2021		<i>ITGB3</i>	Upregulated	Upregulated	(21,22)	
Sanmukh <i>et al</i> , 2018; Sanmukh <i>et al</i> , 2021		<i>ITGB5</i>	Upregulated	Upregulated	(21,22)	
Sanmukh <i>et al</i> , 2018; Sanmukh <i>et al</i> , 2021		<i>MAPK1</i>	Upregulated	Data not available	(21,22)	
Sanmukh <i>et al</i> , 2018; Sanmukh <i>et al</i> , 2021		<i>MAPK3</i>	Upregulated	Data not available	(21,22)	
Sanmukh <i>et al</i> , 2018; Sanmukh <i>et al</i> , 2021		<i>PGC1A</i>	Downregulated	Data not available	(21,22)	
Sanmukh <i>et al</i> , 2018; Sanmukh <i>et al</i> , 2021		<i>PI3K</i>	Upregulated	Data not available	(21,22)	
Sanmukh <i>et al</i> , 2018; Sanmukh <i>et al</i> , 2021		<i>STAT3</i>	Upregulated	Data not available	(21,22)	
Sanmukh <i>et al</i> , 2018; Sanmukh <i>et al</i> , 2021		M13 phage	<i>AKT</i>	Upregulated	Upregulated	(21,22)
Sanmukh <i>et al</i> , 2018; Sanmukh <i>et al</i> , 2021			<i>AR</i>	Downregulated	Downregulated	(21,22)
Sanmukh <i>et al</i> , 2017; Sanmukh <i>et al</i> , 2018; Sanmukh <i>et al</i> , 2021			<i>HSP90</i>	No alteration	Downregulated	(19,21,22)
Sanmukh <i>et al</i> , 2018; Sanmukh <i>et al</i> , 2021			<i>HSP27</i>	No alteration	Downregulated	(21,22)
Sanmukh <i>et al</i> , 2018; Sanmukh <i>et al</i> , 2021			<i>ITGA5</i>	Upregulated	Upregulated	(21,22)
Sanmukh <i>et al</i> , 2018; Sanmukh <i>et al</i> , 2021			<i>ITGAV</i>	No alteration	Upregulated	(21,22)
Sanmukh <i>et al</i> , 2018; Sanmukh <i>et al</i> , 2021	<i>ITGB1</i>		Upregulated	No alteration	(21,22)	
Sanmukh <i>et al</i> , 2018; Sanmukh <i>et al</i> , 2021	<i>ITGB3</i>		Upregulated	Upregulated	(21,22)	
Sanmukh <i>et al</i> , 2018; Sanmukh <i>et al</i> , 2021	<i>ITGB5</i>		Upregulated	Upregulated	(21,22)	
Sanmukh <i>et al</i> , 2018; Sanmukh <i>et al</i> , 2021	<i>MAPK1</i>		Upregulated	Data not available	(21,22)	
Sanmukh <i>et al</i> , 2018; Sanmukh <i>et al</i> , 2021	<i>MAPK3</i>		Upregulated	Data not available	(21,22)	
Sanmukh <i>et al</i> , 2018; Sanmukh <i>et al</i> , 2021	<i>PGC1A</i>		Downregulated	Data not available	(21,22)	
Sanmukh <i>et al</i> , 2018; Sanmukh <i>et al</i> , 2021	<i>PI3K</i>		Upregulated	Data not available	(21,22)	
Sanmukh <i>et al</i> , 2018; Sanmukh <i>et al</i> , 2021	<i>STAT3</i>	Upregulated	Data not available	(21,22)		
Present study	MS2 phage	<i>AKT</i>	Upregulated	Data not available	-	
Present study		<i>AR</i>	Upregulated	Data not available	-	
Present study		<i>HSP90</i>	No alteration	Data not available	-	
Present study		<i>HSP27</i>	No alteration	Data not available	-	
Present study		<i>ITGA5</i>	Upregulated	Data not available	-	
Present study		<i>ITGAV</i>	No alteration	Data not available	-	
Present study		<i>ITGB1</i>	Upregulated	Data not available	-	
Present study		<i>ITGB3</i>	No alteration	Data not available	-	
Present study		<i>ITGB5</i>	No alteration	Data not available	-	
Present study		<i>MAPK1</i>	Upregulated	Data not available	-	
Present study	<i>MAPK3</i>	Upregulated	Data not available	-		
Present study	<i>PGC1A</i>	Upregulated	Data not available	-		
Present study	<i>PI3K</i>	No alteration	Data not available	-		
Present study	<i>STAT3</i>	Upregulated	Data not available	-		

AR, androgen receptor; *HSP27*, heat shock protein 27; *HSP90*, heat shock protein 90; *ITGA5*, integrin $\alpha 5$; *ITGAV*, integrin αV ; *ITGB1*, integrin $\beta 1$; *ITGB3*, integrin $\beta 3$; *ITGB5*, integrin $\beta 5$; *PGC1A*, peroxisome proliferator-activated receptor- γ coactivator 1 α .

Table III. Effect of interaction between bacteriophages and prostate cancer cell lines.

First author/s, year	Interacting bacteriophage	Effect on cancer cell lines	LNCaP cells	PC3 cells	(Refs.)
Kantoch and Mordarski, 1958; Hart <i>et al.</i> , 1994; Tobia <i>et al.</i> , 2012; Dąbrowska <i>et al.</i> , 2014; Sanmukh <i>et al.</i> , 2017 Sanmukh <i>et al.</i> , 2021; Sanmukh <i>et al.</i> , 2021	T4 phage	Phage binding	Yes	Yes	(20,72-75)
Kantoch, 1958; Lehti <i>et al.</i> , 2017; Porayath <i>et al.</i> , 2018; Sanmukh <i>et al.</i> , 2017		Morphology	No significant alteration	Marked alteration (spindle shaped cell formation)	(22,23)
Bloch, 1940; Szczaurska-Nowak <i>et al.</i> , 2009; Dabrowska <i>et al.</i> , 2009; Kurzepa-Skaradzinska <i>et al.</i> , 2013; Sanmukh <i>et al.</i> , 2017; Sanmukh <i>et al.</i> , 2021		Cell proliferation	Reduced	Reduced	(20,76-78)
Merril <i>et al.</i> , 1972; Eriksson <i>et al.</i> , 2009; Sanmukh <i>et al.</i> , 2021		Migration/ invasion	Restricted	Restricted	(20,22,79-82)
Kantoch and Mordarski, 1958; Dąbrowska <i>et al.</i> , 2014; Sanmukh <i>et al.</i> , 2017 Sanmukh <i>et al.</i> , 2021; Sanmukh <i>et al.</i> , 2021	M13 phage	Cell viability	Decreased during initial 4 h	Data not available	(23,83,84)
Kantoch, 1958; Lehti <i>et al.</i> , 2017; Porayath <i>et al.</i> , 2018; Sanmukh <i>et al.</i> , 2017		Phage binding	Yes	Yes	(20,72-75)
Bloch, 1940; Szczaurska-Nowak <i>et al.</i> , 2009; Dabrowska <i>et al.</i> , 2009; Kurzepa-Skaradzinska <i>et al.</i> , 2013; Sanmukh <i>et al.</i> , 2017; Sanmukh <i>et al.</i> , 2021		Morphology	No significant alteration	Marked alteration (spindle shaped cell formation)	(22,23)
Merril <i>et al.</i> , 1972; Eriksson <i>et al.</i> , 2009; Sanmukh <i>et al.</i> , 2021		Cell proliferation	Reduced	Reduced	(20,76-78)
		Migration/ invasion	Restricted	Restricted	(20,22,79-82)
		Cell viability	Decreased during initial 24 h	Data not available	(23,83,84)

transmembrane proteins, such as CD97, CD87, and CD154, contain these tripeptides, thus $\alpha 5\beta 1$ interacts with them and contributes to adhesion, intracellular signaling, angiogenesis, chemotherapy, and radiation resistance (48).

The $\alpha 5$ integrin has also been associated with bone metastasis in breast cancer due to its upregulation, which is considered an important factor contributing to mortality and morbidity in patients with breast cancer (49). Similarly, gene knockout studies of $\beta 1$ integrins in MDA-MB-231 breast

cancer cells have shown that they increase EGFR phosphorylation and decrease AKT phosphorylation, suggesting that they are involved in AKT signaling (50,51). Furthermore, $\alpha 5\beta 1$ integrin maintains pro-survival signaling through continuous AKT activation and upregulates proliferation through EGFR activation in squamous cell carcinomas (47-52).

Upregulation of *MAPK1* and *MAPK3* after bacteriophage MS2 interaction shows that autophagy and compensatory signaling pathways, such as the Ras/Raf/MEK/ERK signaling

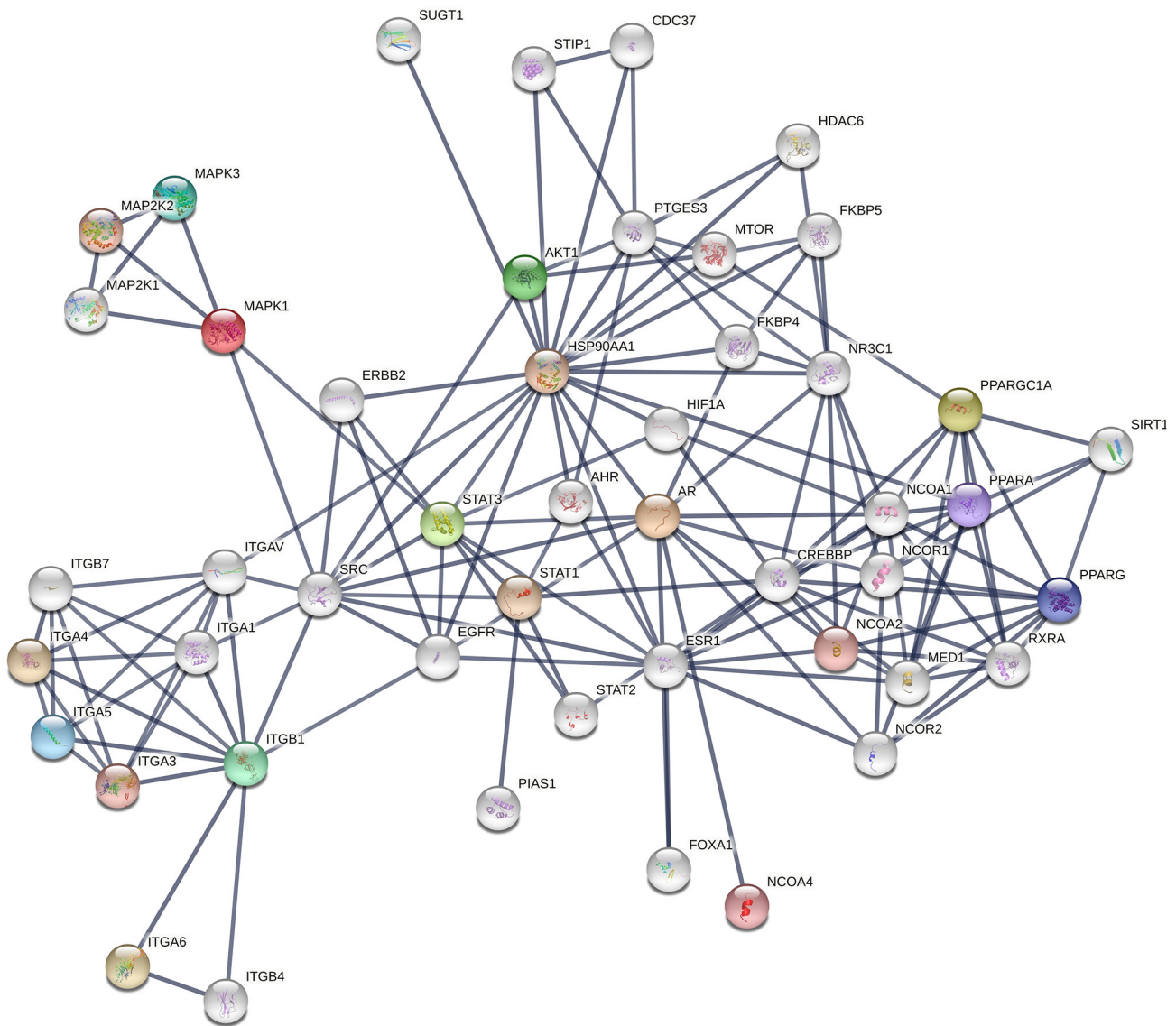


Figure 4. Network of protein-protein interactions in LNCaP cells after their interaction with MS2 bacteriophages. SRC kinases seem to be strongly co-associated with integrins and other associated proteins with the highest level of confidence (0.7-0.9) based on known interactions.

pathway, are activated in LNCaP cancer cells (52,53). Mammalian DNA and RNA viruses have previously been reported to markedly influence the MAPK-ERK cascade through various cellular receptors, which are also regulated by G proteins (53,54). Therefore, targeting the PI3K/AKT/mTOR and Ras/MEK/ERK/FGF signaling pathways together is recommended in prostate cancer and other types of cancer, such as breast cancer (52-55). Direct effects of DNA and RNA viruses on cellular signaling cascades were previously reported; therefore, the effects of bacteriophages T4, M13, and MS2 on gene expression changes in PC3 and LNCaP cell lines cannot be ignored (22,23). In addition, since *MAPK* upregulation is associated with castration-resistant PCa, it is recommended to target the FGF/MAPK signaling pathways in AR-independent PCa to effectively combat PCa metastasis (36-38,52-55).

Upregulation of *PGC1A* is associated with PCa growth and metastasis, regulating estrogen receptor α (ERR α)-dependent transcripts, and is responsible for suppressing metastasis (56). Since *PGC1A*-ERR α contributes to disease stratification (56)

and treatment, these findings are critical for the development of phage-based treatment therapies. The bacteriophages T4, M13 and MS2, when separately used for the treatment of PC3 and LNCaP cells, affected cell viability and *PGC1A* gene expression, which demonstrates the direct effect on mitochondrial function/biogenesis and requires further investigation for the development of phage-based therapies against prostate cancer (56).

Finally, the upregulation of *STAT3* is directly related to the progression of metastasis (57), while its inhibition promotes apoptosis in PCa (58). The expression of *STAT3* and basic FGF (which is a potent angiogenic regulator) are also coregulated, which has been confirmed by gene knockout studies and further validates the FGF/MAPK signaling pathway as a target in AR-independent PCa (59-62).

In addition, the Enrichr server (<https://maayanlab.cloud/Enrichr/>), which is used for large-scale enrichment analysis of gene sets, was used to predict potential bacteriophage entry pathways from upregulated genes in LNCaP cells (27).

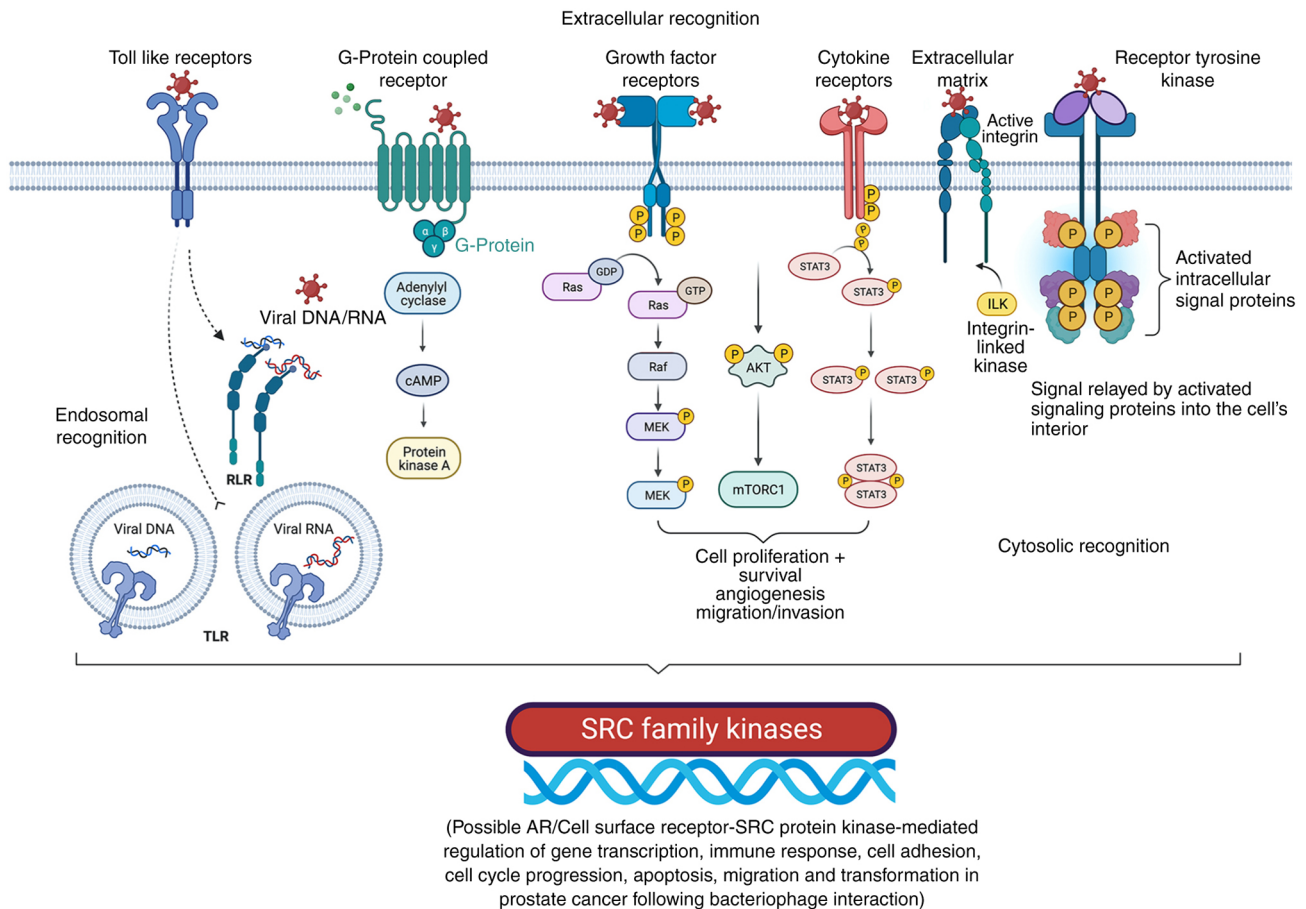


Figure 5. Cell surface receptor-mediated interaction with bacteriophages is associated with SRC family kinases involved in cancer progression, gene upregulation, and other cellular events. Bacteriophages may interact with various cell membrane receptors. Cell surface receptors, such as Toll-like receptors, G-protein coupled receptors, growth factor receptors, cytokine receptors, extracellular matrix (e.g., integrins), and receptor tyrosine kinases could be involved in phage interactions with cancer cells and are responsible for the extracellular recognition of bacteriophages. Following different routes of internalization (e.g., endocytosis), bacteriophages appear to have endosomal recognition. In addition, cytosolic recognition of bacteriophages within cancer cells after degradation/decay of the phage proteins and the genome (DNA/RNA) is possible. Adapted from 'Non-phagocytic Nanoparticle internalization pathways', by BioRender.com (2022). Retrieved from <https://app.biorender.com/illustrations/62e7f61bf2dd732bb630d9eb>. P, phosphate group; AR, androgen receptor; ILK, integrin-linked kinase; TLR, toll-like receptors.

In this prediction, 'caveolin-mediated endocytosis' was the entry pathway for bacteriophage MS2 ($P=0.000001399$; Fig. S1) based on upregulation of *AKT*, *AR*, *ITGA5*, *ITGB1*, *MAPK1*, *MAPK3*, *PGC1A*, and *STAT3* genes (27,44-46). This prediction also fits well with the bacteriophage MS2 size scale (23-28 nm) as the caveolin-mediated endocytic process involves 50-60 nm tuberos invaginations of the plasma membrane, named 'caveolae' (small cavities), which are the best possible mode as far as the size is concerned for bacteriophage MS2 internalization (27,44-46). The mechanisms underlying these effects require further experimental validation. Similarly, bacteriophage M13 is reported to get internalized through clathrin-dependent endocytosis, which has a larger dimension (880 nm in length and 6 nm in diameter) (34). But, through GO biological processes Enrichr web server-based gene set enrichment analysis for upregulated cancer progression genes in LNCaP cells treated with bacteriophages T4 and M13, 'integrin-mediated signaling pathway' ($P=0.000007588$) and 'caveolin-mediated endocytosis' ($P=0.000001799$) were predicted for both these bacteriophages based on the upregulated gene sets of *AKT*, *ITGA5*, *ITGB1*, *ITGB3*, *ITGB5*, *MAPK1*, *MAPK3*, *PI3K*, and

STAT3 genes. The gene set analysis was performed based on overexpressed genes in LNCaP cells from our studies to predict GO biological processes. Similarly, through GO cellular component prediction focal adhesion, cell-substrate junction, caveola, plasma membrane raft, early and late endosomes were predicted for MS2, T4, as well as M13 phages validating the caveolin-mediated endocytosis for these phages. Bacteriophage MS2 internalization in cancer cells through caveolin-mediated endocytosis was predicted based on the results of the present study, as shown in Fig. 6, which also confirmed previous reports (11,27,44-46).

Phage display library screening has attracted attention as an inexpensive method for drug discovery (63). Several short peptides presented on the surface of phages against, for example, a membrane receptor, offer a much larger scale analysis compared with synthetic peptide libraries (63-65). This number can be further increased when considering non-peptide mimetics designed based on these short peptides. This is particularly important in oncology drug development, where large-scale drug screening is required due to a variety of different drug targets and signaling pathways that may simultaneously be involved in tumor growth and progression (63-65).

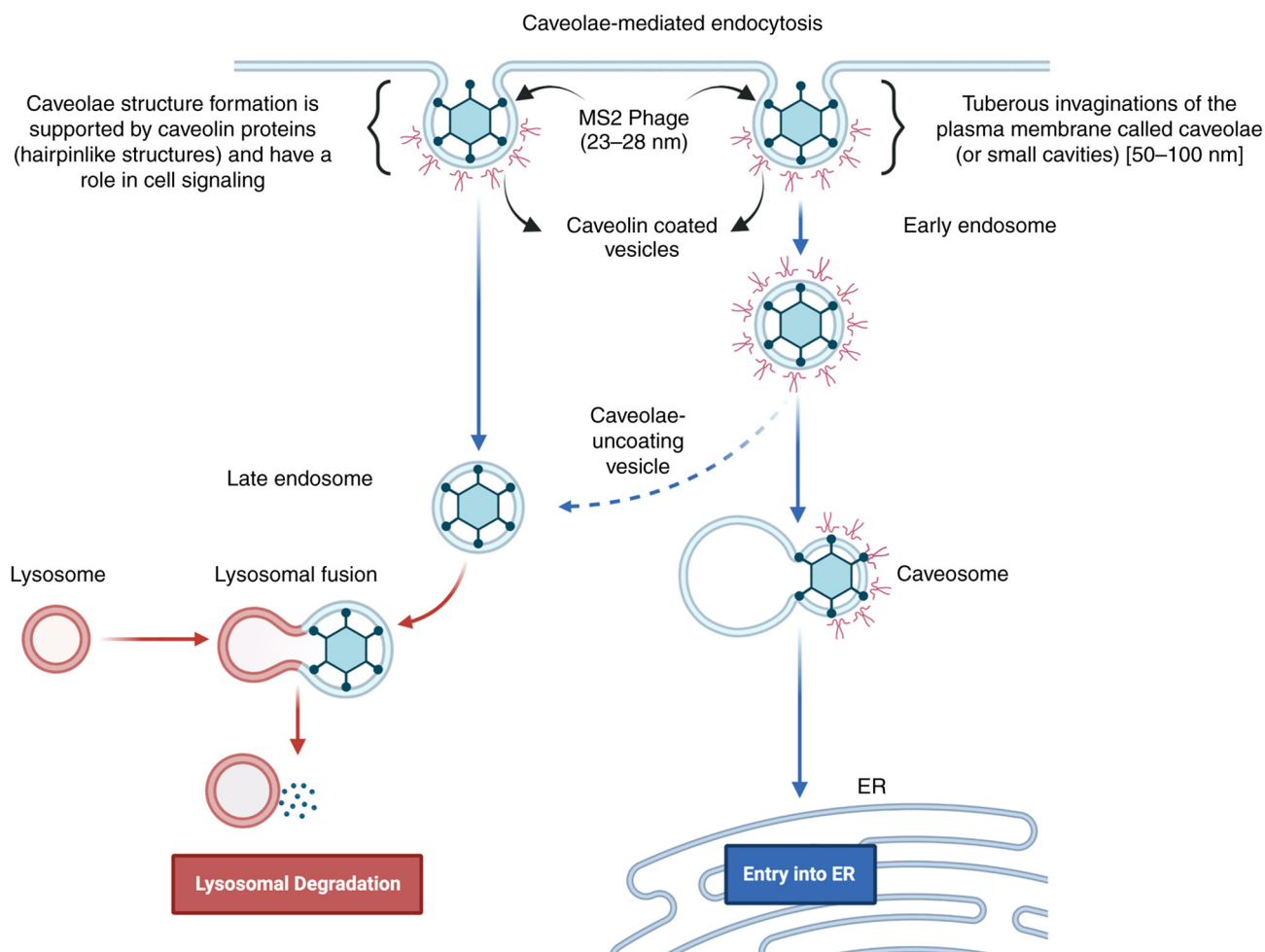


Figure 6. Representation of caveolin-mediated endocytosis for bacteriophage MS2 as a possible phage internalization mechanism. Adapted from 'Innate Immune System: Cellular Locations of Pattern Recognition Receptors', by BioRender.com (2022). Retrieved from <https://app.biorender.com/illustrations/63a1fec6c1fcc7da85a8ae0>.

Based on the early report of bacteriophage lambda-holin protein reducing tumor growth rates in mammary cancer cell xenograft models (64), it appears that phages and phage proteins may be useful for cancer gene therapy.

Similarly, GPCR drug targets involved in cancer include lysophosphatidic acid receptors (LPA1-6; involved in Rho-dependent signaling pathways) (31,65-67), protease-activated receptors (involved in Hippo/yes-associated protein 1 signaling pathways and angiogenesis) (68), frizzled receptors, parathyroid hormone 1 receptor (involved in the Wnt signaling pathway), chemokine receptors (69), endothelin receptors (involved in crosstalk with EGFR and β -catenin stabilization), prostaglandin receptors (involved in the cyclooxygenase pathway), bradykinin receptors (involved in crosstalk with EGFR, Ras, Raf, and ERK), sphingosine receptor 1 phosphate (involved in crosstalk with Ras-ERK, PI3K/Akt/Rac, Rho and STAT3), angiotensin II receptor type 1 (involved in crosstalk with TNF- α , ERK1/2, NF- κ B, STAT) and gastrin-releasing peptide receptor (involved in crosstalk with NF- κ B, p38-MAPK and PI3K/AKT), which are among the most commonly targeted in cases of PCa (63,70-72). Adhesion GPCRs, which until recently had not been extensively studied in terms of structure and ligand determination, serve an important

role in regulating cell adhesion, migration, proliferation, and tumor survival (31,66,67). Peptide libraries containing phage display peptides have been used to target LPA1 receptors (65), protease-activated (69), chemokine (69), frizzled (70,71) and sphingosine 1-phosphate receptor 1 (72).

The importance of phage-displayed peptides in phage engineering, the natural peptide display effect of bacteriophage MS2 observed in the present study, and previous studies of bacteriophages T4 and M13 (20-23) suggest that along with other adjuvant therapies, targeting adhesion GPCRs, integrins and other receptors appear to be effective against multiple types of cancer, including ovarian, breast and prostate cancer (31,66,67). Phages can be engineered to express surface peptides and transport cargo, making them prime candidates for fighting cancer, due to their ubiquity (10,63,73,74).

In conclusion, the natural bacteriophage MS2 interacts directly with LNCaP cells and their surface receptors to induce marked changes in gene expression in LNCaP cancer cells. This, in turn, affects the viability of LNCaP cells. As such interactions have been demonstrated to affect cancer cell metabolism and direct gene expression, upregulation of the AR, AKT and MAPK genes suggests that these genes affected the AR, AKT, and MAPK signaling pathways (23). Such effects may be beneficial in light of existing therapies

that target the inhibitors of the AKT/MAPK/FGF signaling pathway. To demonstrate that bacteriophage MS2 is effective in fighting PCa, further studies are needed to analyze and display modified phage surface peptides against cancer cell receptors and proteins, such as G-proteins, GPCRs, and integrins. Based on previous reports that analyzed the interactions between DNA phages (T4 and M13) (20-23) and the present study which demonstrated the interaction between RNA (MS2) phages with LNCaP cells, it can be concluded that phages, specifically MS2, utilize caveolin-mediated endocytosis and alter PCa cell signaling pathways. The wide range of applications against antibiotic-resistant bacterial pathogens makes phage engineering an ideal technique for simultaneously targeting cancer cells and antibiotic-resistant bacterial pathogens.

Acknowledgments

The article is part of a Ph.D. thesis developed by SGS at the Institute of Biosciences of Botucatu, Sao Paulo State University (Botucatu, Brazil).

Funding

Funding was received from the National Council for Scientific and Technological Development (CNPq; grant nos. 465699/2014-6 and 310805/2018-0) and São Paulo Research Foundation (FAPESP; grant nos. 2014/50938-8 and 2019/19644-1). The present study was also carried out with the support of the Coordenação de Aperfeiçoamento de Pessoal de Nível Superior, Brasil (CAPES; finance code 001; grant no. 963-14-2).

Availability of data and materials

All data generated or analyzed during this study are included in this published article.

Authors' contributions

SGS conducted most of the experiments and analyses. SGS, NJDS, CNB, and MDC generated data/performed analyses. SGS, NJDS, CNB, MDC, PPDR, FKD, HFC, DL, TF, and SLF confirm the authenticity of all the raw data. SGS and SLF drafted the manuscript. FKD, PPDR, and SLF supervised the project. FKD, HFC, DL, TF, and SLF were responsible for overseeing the manuscript. SGS, NJDS, CNB, PPDR, FKD, HFC, DL, TF, and SLF were responsible for writing and revising the manuscript and contributed significantly to the study design, data collection, data analysis, and interpretation of data. All authors read and approved the final version of the manuscript.

Ethics approval and consent to participate

Not applicable.

Patient consent for publication

Not applicable.

Competing interests

The authors declare that they have no competing interests.

References

1. Bray F, Ferlay J, Soerjomataram I, Siegel RL, Torre LA and Jemal A: Global cancer statistics 2018: GLOBOCAN estimates of incidence and mortality worldwide for 36 cancers in 185 countries. *CA Cancer J Clin* 68: 394-424, 2018.
2. Siegel RL, Miller KD, Fuchs HE and Jemal A: Cancer statistics, 2021. *CA Cancer J Clin* 71: 7-33, 2021.
3. Sakr WA, Grignon DJ, Crissman JD, Heilbrun LK, Cassin BJ, Pontes JJ and Haas GP: High grade prostatic intraepithelial neoplasia (HGPIN) and prostatic adenocarcinoma between the ages of 20-69: An autopsy study of 249 cases. *In Vivo* 8: 439-443, 1994.
4. Nelson WG, De Marzo AM and Isaacs WB: Prostate cancer. *N Engl J Med* 349: 366-381, 2003.
5. Nuhn P, De Bono JS, Fizazi K, Freedland SJ, Grilli M, Kantoff PW, Sonpavde G, Sternberg CN, Yegnasubramanian S and Antonarakis ES: Update on systemic prostate cancer therapies: Management of metastatic castration-resistant prostate cancer in the era of precision oncology. *Eur Urol* 75: 88-99, 2019.
6. Sumanasuriya S and De Bono J: Treatment of advanced prostate cancer-a review of current therapies and future promise. *Cold Spring Harb Perspect Med* 8: a030635, 2018.
7. Barquilha CN, Santos NJ, Monção CCD, Barbosa IC, Lima FO, Justulin LA, Pértega-Gomes N and Felisbino SL: Sulfiredoxin as a potential therapeutic target for advanced and metastatic prostate cancer. *Oxid Med Cell Longev* 2020: 2148562, 2020.
8. Przystal JM, Waramit S, Pranjol MZI, Yan W, Chu G, Chongchai A, Samarth G, Olaciregui NG, Tabatabai G, Carcaboso AM, *et al.*: Efficacy of systemic temozolomide-activated phage-targeted gene therapy in human glioblastoma. *EMBO Mol Med* 11: e8492, 2019.
9. Ren S, Fengyu, Zuo S, Zhao M, Wang X, Wang X, Chen Y, Wu Z and Ren Z: Inhibition of tumor angiogenesis in lung cancer by T4 phage surface displaying mVEGFR2 vaccine. *Vaccine* 29: 5802-5811, 2011.
10. Shadidi M, Sørensen D, Dybwad A, Furset G and Sioud M: Mucosal vaccination with phage-displayed tumour antigens identified through proteomics-based strategy inhibits the growth and metastasis of 4T1 breast adenocarcinoma. *Int J Oncol* 32: 241-247, 2008.
11. Ashley CE, Carnes EC, Phillips GK, Durfee PN, Buley MD, Lino CA, Padilla DP, Phillips B, Carter MB, Willman CL, *et al.*: Cell-specific delivery of diverse cargos by bacteriophage MS2 virus-like particles. *ACS Nano* 5: 5729-5745, 2011.
12. Aanei IL, ElSohly AM, Farkas ME, Netirojjanakul C, Regan M, Taylor Murphy S, O'Neil JP, Seo Y and Francis MB: Biodistribution of antibody-MS2 viral capsid conjugates in breast cancer models. *Mol Pharm* 13: 3764-3772, 2016.
13. Li J, Sun Y, Jia T, Zhang R, Zhang K and Wang L: Messenger RNA vaccine based on recombinant MS2 virus-like particles against prostate cancer. *Int J Cancer* 134: 1683-1694, 2014.
14. Zhai L, Yadav R, Kunda NK, Anderson D, Bruckner E, Miller EK, Basu R, Muttli P and Tumban E: Oral immunization with bacteriophage MS2-L2 VLPs protects against oral and genital infection with multiple HPV types associated with head & neck cancers and cervical cancer. *Antiviral Res* 166: 56-65, 2019.
15. Lino CA, Caldeira JC and Peabody DS: Display of single-chain variable fragments on bacteriophage MS2 virus-like particles. *J Nanobiotechnology* 15: 13, 2017.
16. Chang L, Wang G, Jia T, Zhang L, Li Y, Han Y, Zhang K, Lin G, Zhang R, Li J and Wang L: Armored long non-coding RNA MEG3 targeting EGFR based on recombinant MS2 bacteriophage virus-like particles against hepatocellular carcinoma. *Oncotarget* 7: 23988-24004, 2016.
17. Briolay T, Petithomme T, Fouet M, Nguyen-Pham N, Blanquart C and Boisgerault N: Delivery of cancer therapies by synthetic and bio-inspired nanovectors. *Mol Cancer* 20: 55, 2021.
18. Kolesanova EF, Melnikova MV, Bolshakova TN, Rybalkina EY and Sivov IG: Bacteriophage MS2 as a tool for targeted delivery in solid tumor chemotherapy. *Acta Naturae* 11: 98-101, 2019.
19. Sanmukh SG and Felisbino SL: Bacteriophages in cancer biology and therapies. *Clin Oncol* 2: 1295, 2017.

20. Sanmukh SG, Dos Santos SAA and Felisbino SL: Natural bacteriophages T4 and M13 down-regulates Hsp90 gene expression in human prostate cancer cells (PC-3) representing a potential nanoparticle against cancer. *Virology Res J* 1: 21-23, 2017.
21. Sanmukh SG and Felisbino SL: Development of pipette tip gap closure migration assay (s-ARU method) for studying semi-adherent cell lines. *Cytotechnology* 70: 1685-1695, 2018.
22. Sanmukh SG, Santos NJ, Barquilha CN, dos Santos SAA, Duran BOS, Delella FK, Moroz A, Justulin LA, Carvalho HF and Felisbino SL: Exposure to bacteriophages T4 and M13 increases integrin gene expression and impairs migration of human PC-3 prostate cancer cells. *Antibiotics (Basel)* 10: 1202, 2021.
23. Sanmukh SG, Dos Santos NJ, Barquilha CN, Cuciello MS, de Carvalho M, Dos Reis PP, Delella FK, Carvalho HF and Felisbino SL: Bacteriophages M13 and T4 increase the expression of anchorage-dependent survival pathway genes and down regulate androgen receptor expression in LNCaP prostate cell line. *Viruses* 13: 1754, 2021.
24. Mosmann T: Rapid colorimetric assay for cellular growth and survival: Application to proliferation and cytotoxicity assays. *J Immunol Methods* 65: 55-63, 1983.
25. Berridge MV and Tan AS: Characterization of the cellular reduction of 3-(4,5-dimethylthiazol-2-yl)-2,5-diphenyltetrazolium bromide (MTT): Subcellular localization, substrate dependence, and involvement of mitochondrial electron transport in MTT reduction. *Arch Biochem Biophys* 303: 474-482, 1993.
26. Livak KJ and Schmittgen TD: Analysis of relative gene expression data using real-time quantitative PCR and the 2(-Delta Delta C(T)) method. *Methods* 25: 402-408, 2001.
27. Xie Z, Bailey A, Kuleshov MV, Clarke DJB, Evangelista JE, Jenkins SL, Lachmann A, Wojciechowicz ML, Kropiwnicki E, Jagodnik KM, *et al*: Gene set knowledge discovery with enrichr. *Curr Protoc* 1: e90, 2021.
28. Szklarczyk D, Gable AL, Nastou KC, Lyon D, Kirsch R, Pyysalo S, Doncheva NT, Legeay M, Fang T, Bork P, *et al*: The STRING database in 2021: Customizable protein-protein networks, and functional characterization of user-uploaded gene/measurement sets. *Nucleic Acids Res* 49 (D1): D605-D612, 2021.
29. Langer I, Jeandriens J, Couvineau A, Sanmukh S and Latek D: Signal transduction by VIP and PACAP receptors. *Biomedicines* 10: 406, 2022.
30. Peterson YK and Luttrell LM: The diverse roles of arrestin scaffolds in G protein-coupled receptor signaling. *Pharmacol Rev* 69: 256-297, 2017.
31. Gad AA and Balenga N: The Emerging Role of adhesion GPCRs in cancer. *ACS Pharmacol Transl Sci* 3: 29-42, 2020.
32. Liscano Y, Oñate-Garzón J and Delgado JP: Peptides with Dual antimicrobial-anticancer activity: Strategies to overcome peptide limitations and rational design of anticancer peptides. *Molecules* 25: 4245, 2020.
33. Hwang JS, Kim SG, Shin TH, Jang YE, Kwon DH and Lee G: Development of anticancer peptides using artificial intelligence and combinational therapy for cancer therapeutics. *Pharmaceutics* 14: 997, 2022.
34. Ripa I, Andreu S, López-Guerrero JA and Bello-Morales R: Membrane rafts: Portals for viral entry. *Front Microbiol* 12: 631274, 2021.
35. Kim A, Shin TH, Shin SM, Pham CD, Choi DK, Kwon MH and Kim YS: Cellular internalization mechanism and intracellular trafficking of filamentous M13 phages displaying a cell-penetrating transbody and TAT peptide. *PLoS One* 7: e51813, 2012.
36. Peterziel H, Mink S, Schonert A, Becker M, Klocker H and Cato AC: Rapid signalling by androgen receptor in prostate cancer cells. *Oncogene* 18: 6322-6329, 1999.
37. Liao RS, Ma S, Miao L, Li R, Yin Y and Raj GV: Androgen receptor-mediated non-genomic regulation of prostate cancer cell proliferation. *Transl Androl Urol* 2: 187-196, 2013.
38. Heinlein CA and Chang C: The roles of androgen receptors and androgen-binding proteins in nongenomic androgen actions. *Mol Endocrinol* 16: 2181-2187, 2002.
39. Siu MK, Chen WY, Tsai HY, Yeh HL, Yin JJ, Liu SY and Liu YN: Androgen receptor regulates SRC expression through microRNA-203. *Oncotarget* 7: 25726-25741, 2016.
40. Taheri M, Khoshbakht T, Jamali E, Kallenbach J, Ghafouri-Fard S and Baniahmad A: Interaction between non-coding RNAs and androgen receptor with an especial focus on prostate cancer. *Cells* 10: 3198, 2021.
41. Kim KH, Dobi A, Shaheduzzaman S, Gao CL, Masuda K, Li H, Drukier A, Gu Y, Srikantan V, Rhim JS and Srivastava S: Characterization of the androgen receptor in a benign prostate tissue-derived human prostate epithelial cell line: RC-165N/human telomerase reverse transcriptase. *Prostate Cancer Prostatic Dis* 10: 30-38, 2007.
42. Zhang J, Li D, Zhang R, Peng R and Li J: Delivery of microRNA-21-sponge and pre-microRNA-122 by MS2 virus-like particles to therapeutically target hepatocellular carcinoma cells. *Exp Biol Med (Maywood)* 246: 2463-2472, 2021.
43. Foglizzo V and Marchiò S: Bacteriophages as therapeutic and diagnostic vehicles in cancer. *Pharmaceutics (Basel)* 14: 161, 2021.
44. Echarri A and Del Pozo MA: Caveolae internalization regulates integrin-dependent signaling pathways. *Cell Cycle* 5: 2179-2182, 2006.
45. Shi F and Sottile J: Caveolin-1-dependent beta1 integrin endocytosis is a critical regulator of fibronectin turnover. *J Cell Sci* 121: 2360-2371, 2008.
46. Tahir SA, Yang G, Ebara S, Timme TL, Satoh T, Li L, Goltsov A, Ittmann M, Morrisett JD and Thompson TC: Secreted caveolin-1 stimulates cell survival/clonal growth and contributes to metastasis in androgen-insensitive prostate cancer. *Cancer Res* 61: 3882-3885, 2001.
47. Xing Y, Wen Z, Gao W, Lin Z, Zhong J and Jiu Y: Multifaceted functions of host cell caveolae/caveolin-1 in virus infections. *Viruses* 12: 487, 2020.
48. Schaffner F, Ray AM and Dontenwill M: Integrin $\alpha 5 \beta 1$, the fibronectin receptor, as a pertinent therapeutic target in solid tumors. *Cancers (Basel)* 5: 27-47, 2013.
49. Hou J, Yan D, Liu Y, Huang P and Cui H: The roles of integrin $\alpha 5 \beta 1$ in human cancer. *Onco Targets Ther* 13: 13329-13344, 2020.
50. Pantano F, Croset M, Driouch K, Bednarz-Knoll N, Iuliani M, Ribelli G, Bonnelye E, Wikman H, Geraci S, Bonin F, *et al*: Integrin alpha5 in human breast cancer is a mediator of bone metastasis and a therapeutic target for the treatment of osteolytic lesions. *Oncogene* 40: 1284-1299, 2021.
51. Hou S, Isaji T, Hang Q, Im S, Fukuda T and Gu J: Distinct effects of $\beta 1$ integrin on cell proliferation and cellular signaling in MDA-MB-231 breast cancer cells. *Sci Rep* 6: 18430, 2016.
52. Morozovich GE, Kozlova NI, Ushakova NA, Preobrazhenskaya ME and Berman AE: Integrin $\alpha 5 \beta 1$ simultaneously controls EGFR-dependent proliferation and Akt-dependent pro-survival signaling in epidermoid carcinoma cells. *Aging (Albany NY)* 4: 368-374, 2012.
53. Butler DE, Marlein C, Walker HF, Frame FM, Mann VM, Simms MS, Davies BR, Collins AT and Maitland NJ: Inhibition of the PI3K/AKT/mTOR pathway activates autophagy and compensatory Ras/Raf/MEK/ERK signalling in prostate cancer. *Oncotarget* 8: 56698-56713, 2017.
54. DuShane JK and Maginnis MS: Human DNA virus exploitation of the MAPK-ERK cascade. *Int J Mol Sci* 20: 3427, 2019.
55. Mukherjee R, McGuinness DH, McCall P, Underwood MA, Seywright M, Orange C and Edwards J: Upregulation of MAPK pathway is associated with survival in castrate-resistant prostate cancer. *Br J Cancer* 104: 1920-1928, 2011.
56. Bluemn EG, Coleman IM, Lucas JM, Coleman RT, Hernandez-Lopez S, Tharakan R, Bianchi-Frias D, Dumpit RF, Kaipainen A, Corella AN, *et al*: Androgen receptor pathway-independent prostate cancer is sustained through FGF signaling. *Cancer Cell* 32: 474-489.e6, 2017.
57. Liang H and Ward WF: PGC-1alpha: A key regulator of energy metabolism. *Adv Physiol Educ* 30: 145-151, 2006.
58. Abdulghani J, Gu L, Dagvadorj A, Lutz J, Leiby B, Bonuccelli G, Lisanti MP, Zellweger T, Alanen K, Mirtti T, *et al*: Stat3 promotes metastatic progression of prostate cancer. *Am J Pathol* 172: 1717-1728, 2008.
59. Barton BE, Karras JG, Murphy TF, Barton A and Huang HF: Signal transducer and activator of transcription 3 (STAT3) activation in prostate cancer: Direct STAT3 inhibition induces apoptosis in prostate cancer lines. *Mol Cancer Ther* 3: 11-20, 2004.
60. Bishop JL, Thaper D and Zoubeidi A: The multifaceted roles of STAT3 signaling in the progression of prostate cancer. *Cancers (Basel)* 6: 829-859, 2014.
61. Zhao M, Gao FH, Wang JY, Liu F, Yuan HH, Zhang WY and Jiang B: JAK2/STAT3 signaling pathway activation mediates tumor angiogenesis by upregulation of VEGF and bFGF in non-small-cell lung cancer. *Lung Cancer* 73: 366-374, 2011.

62. Kujawski M, Kortylewski M, Lee H, Herrmann A, Kay H and Yu H: Stat3 mediates myeloid cell-dependent tumor angiogenesis in mice. *J Clin Invest* 118: 3367-3377, 2008.
63. Molek P, Strukelj B and Bratkovic T: Peptide phage display as a tool for drug discovery: Targeting membrane receptors. *Molecules* 16: 857-887, 2011.
64. Agu CA, Klein R, Schwab S, König-Schuster M, Kodajova P, Ausserlechner M, Binischofer B, Bläsi U, Salmons B, Günzburg WH and Hohenadl C: The cytotoxic activity of the bacteriophage lambda-holin protein reduces tumour growth rates in mammary cancer cell xenograft models. *J Gene Med* 8: 229-241, 2006.
65. David M, Ribeiro J, Descotes F, Serre CM, Barbier M, Murone M, Clézardin P and Peyruchaud O: Targeting lysophosphatidic acid receptor type 1 with Debio 0719 inhibits spontaneous metastasis dissemination of breast cancer cells independently of cell proliferation and angiogenesis. *Int J Oncol* 40: 1133-1141, 2012.
66. Chaudhary PK and Kim S: An insight into GPCR and G-proteins as cancer drivers. *Cells* 10: 3288, 2021.
67. Bar-Shavit R, Maoz M, Kancharla A, Nag JK, Agranovich D, Grisaru-Granovsky S and Uziely B: G protein-coupled receptors in cancer. *Int J Mol Sci* 17: 1320, 2016.
68. Yang J, Mapelli C, Wang Z, Sum CS, Hua J, Lawrence RM, Ni Y and Seiffert DA: An optimized agonist peptide of protease-activated receptor 4 and its use in a validated platelet-aggregation assay. *Platelets* 33: 979-986, 2022.
69. Hu Y, Ma A, Lin S, Yang Y and Hong G: Novel peptide screened from a phage display library antagonizes the activity of CC chemokine receptor 9. *Oncol Lett* 14: 6471-6476, 2017.
70. Nickho H, Younesi V, Aghebati-Maleki L, Motallebnezhad M, Majidi Zolbanin J, Movassagh Pour A and Yousefi M: Developing and characterization of single chain variable fragment (scFv) antibody against frizzled 7 (Fzd7) receptor. *Bioengineered* 8: 501-510, 2017.
71. Pavlovic Z, Adams JJ, Blazer LL, Gakhal AK, Jarvik N, Steinhart Z, Robitaille M, Mascall K, Pan J, Angers S, *et al*: A synthetic anti-frizzled antibody engineered for broadened specificity exhibits enhanced anti-tumor properties. *MAbs* 10: 1157-1167, 2018.
72. Tobia C, Chiodelli P, Nicoli S, Dell'era P, Buraschi S, Mitola S, Foglia E, van Loenen PB, Alewijnse AE and Presta M: Sphingosine-1-phosphate receptor-1 controls venous endothelial barrier integrity in zebrafish. *Arterioscler Thromb Vasc Biol* 32: e104-e116, 2012.
73. Dąbrowska K, Kaźmierczak Z, Majewska J, Miernikiewicz P, Piotrowicz A, Wietrzyk J, Lecion D, Hodyra K, Nasulewicz-Goldeman A, Owczarek B and Górski A: Bacteriophages displaying anticancer peptides in combined antibacterial and anticancer treatment. *Future Microbiol* 9: 861-869, 2014.
74. Hart SL, Knight AM, Harbottle RP, Mistry A, Hunger HD, Cutler DF, Williamson R and Coutelle C: Cell binding and internalization by filamentous phage displaying a cyclic Arg-Gly-Asp-containing peptide. *J Biol Chem* 269: 12468-12474, 1994.
75. Kantoch M and Mordarski M: Binding of bacterial viruses by cancer cells in vitro. *Postepy Hig Med Dosw* 12: 191-192, 1958.
76. Porayath C, Salim A, Palillam Veedu A, Babu P, Nair B, Madhavan A and Pal S: Characterization of the bacteriophages binding to human matrix molecules. *Int J Biol Macromol* 110: 608-615, 2018.
77. Lehti TA, Pajunen MI, Skog MS and Finne J: Internalization of a polysialic acid-binding Escherichia coli bacteriophage into eukaryotic neuroblastoma cells. *Nat Commun* 8: 1915, 2017.
78. Kantoch M: Studies on phagocytosis of bacterial viruses. *Arch Immunol Ther Exp* 6: 63-84, 1958.
79. Bloch H: Experimental investigation on the relationships between bacteriophages and malignant tumors. *Arch Virol* 1: 481-496, 1940 (In German).
80. Szczauńska-Nowak K, Dąbrowska K, Celka M, Kurzepa A, Nevozhay D, Wietrzyk J, Swiatała-Jelen K, Syper D, Pozniak G, Opolski A, *et al*: Antitumor effect of combined treatment of mice with cytostatic agents and bacteriophage T4. *Anticancer Res* 29: 2361-2370, 2009.
81. Dąbrowska K, Skaradziński G, Jończyk P, Kurzepa A, Wietrzyk J, Owczarek B, Zaczek M, Swiatała-Jeleń K, Boratyński J, Poźniak G, *et al*: The effect of bacteriophages T4 and HAP1 on in vitro melanoma migration. *BMC Microbiol* 9: 13, 2009.
82. Kurzepa-Skaradzinska A, Skaradzinski G, Weber-Dąbrowska B, Zaczek M, Maj T, Sławek A, Swiatałska M, Maciejewska M, Wietrzyk J, Rymowicz W and Gorski A: Influence of bacteriophage preparations on migration of HL-60 leukemia cells in vitro. *Anticancer Res* 33: 1569-1574, 2013.
83. Merrill CR, Friedman TB, Attallah AF, Geier MR, Krell K and Yarkin R: Isolation of bacteriophages from commercial sera. *In Vitro* 8: 91-93, 1972.
84. Eriksson F, Tsagozis P, Lundberg K, Parsa R, Mangsbo SM, Persson MA, Harris RA and Pisa P: Tumor-specific bacteriophages induce tumor destruction through activation of tumor-associated macrophages. *J Immunol* 182: 3105-3111, 2009.



This work is licensed under a Creative Commons Attribution-NonCommercial-NoDerivatives 4.0 International (CC BY-NC-ND 4.0) License.